AIAA JOURNAL
Vol. 44, No. 1, January 2006

Pulsed-Laser-Induced Vibration of Pressurized Thin-Walled Cylinder

Harold Mirels* and Kevin L. Zondervan†
The Aerospace Corporation, El Segundo, California 90245-4691

Vibrations of a thin-walled pressurized cylinder, because of impulse loading induced by a high-energy pulsed laser beam, are investigated. Differential equations that describe cylinder oscillations for the case where variations in the axial direction are negligible are presented. The fluence profile of the incident beam is also assumed not to vary in the axial direction. Analytic expressions that provide the frequency and amplitude of the harmonic vibrational modes are derived. The computation of the laser-induced strain perturbation requires a numerical summation. Numerical results for induced hoop strain are given for both uniform and Gaussian beams.

Nomenclature

a	=	cylinder radius; Fig. 1
a_n	=	Fourier coefficient; Eq. (22a)
C	=	coupling coefficient; Eq. (11b)
E	=	modulus of elasticity
E'	=	effective modulus of elasticity; Eq. (2c)
F, F_0	=	laser fluence; Fig. 1 and Eq. (11b)
$f(\theta)$	=	laser fluence profile; Eq. (12)
h	=	cylinder thickness; Fig. 1
N	=	characteristic mode number; Eq. (10)
n	=	mode number; Eq. (3)
p	=	cylinder internal pressure
s	=	incident net beam width; Fig. 1
t	=	time
V	=	center-of-mass velocity; Eq. (13a)
v, w	=	circumferential and radial perturbations; Fig. 1
w_c	=	characteristic radial perturbation; Eq. (14a)
ε	=	hoop strain perturbation; Eq. (A2)
ε_i	=	parameter related to initial pressure-induced hoop strain; Eq. (2a)
θ	=	cylinder angle coordinate; Fig. 1
θ_s	=	angle corresponding to edge of incident beam; Eq. (11d)
ν	=	Poisson's ratio
ρ	=	wall density
σ	=	hoop stress perturbation; Appendix A
σ_i	=	initial pressure-induced hoop stress; Eq. (1)
τ	=	normalized time; Eq. (14a)
Φ	=	normalized center-of-mass velocity; Eq. (13b)
ψ	=	beam width and pressure effect parameter; Eq. (40)
Ω	=	normalized frequency; Eq. (14a)
ω	=	frequency; Eq. (3)
ω_0	=	reference frequency; Eq. (2c)

Subscripts

m	=	local maximum value; Table 1
$0, 1, \ldots, n$	=	mode number; Eq. (3)

Superscripts

$+$	=	extensional mode; Eqs. (7)
$-$	=	inextensional mode; Eqs. (8)

Received 16 June 2004; presented as Paper 2005-747 at the AIAA 43rd Aerospace Sciences Meeting, Reno, NV, 10–13 January 2005; revision received 13 June 2005; accepted for publication 22 June 2005.

*Principal Scientist, Space Based Surveillance Division, Space Program Operations. Fellow AIAA.

†Systems Director, Missile Defense Division, Systems Planning and Engineering. Senior Member AIAA.

I. Introduction

THE interaction between a high-energy laser pulse and a surface can result in material blowoff and impulse loading. The latter can induce vibration, which can, in turn, lead to structural damage or failure. As a result, high-energy pulsed lasers are often considered as a component of a missile defense system.[1]

Research in the area of pulsed-laser surface interaction has focused on the determination of the laser levels needed to induce blowoff and determination of the coupling coefficient that relates incident fluence to impulse.[1] The subsequent effect on the structure has received less attention. In this connection, Sutton[2] has evaluated the wall vibration induced in a pressurized cylinder by a high-energy laser pulse of uniform width and infinite axial extent (i.e., a "slab" beam). However, Sutton's model neglects curvature effects, which, in fact, play a significant role in the structural response for beam widths of the order of the cylinder diameter. Hence, a study of the vibrational response of a gas-pressurized cylinder, to a high-energy laser pulse, including curvature effects, was undertaken. Initial results have been presented in Ref. 3. There, upper-bound estimates were given for the maximum stress induced by a uniform profile slab beam with a width s that was equal to or considerably smaller than the cylinder diameter $2a$. In the present study, following Ref. 4, we provide analytic expressions for the amplitude and frequency of the harmonic modes, for arbitrary beam width and slab-beam profile. These permit the evaluation of the laser-induced strain perturbation as a function of location and time. Numerical results are given for both uniform and Gaussian beams and are compared with those in Ref. 2. Finally, the effect of pressure level and laser beam width on the nature of the vibration is discussed.

II. Analysis

We consider wall vibrations of a gas-pressurized cylinder of radius a, axial length L, thickness h, internal pressure p, and wall density ρ (Fig. 1) and assume h/a and $a/L \ll 1$.

The initial pressure-induced hoop stress σ_i is

$$\sigma_i = pa/h \tag{1}$$

Let w and v denote small displacements in the radial and tangential directions, respectively, of points on the midsection of the pressurized cylinder wall. These are functions of the initial angular

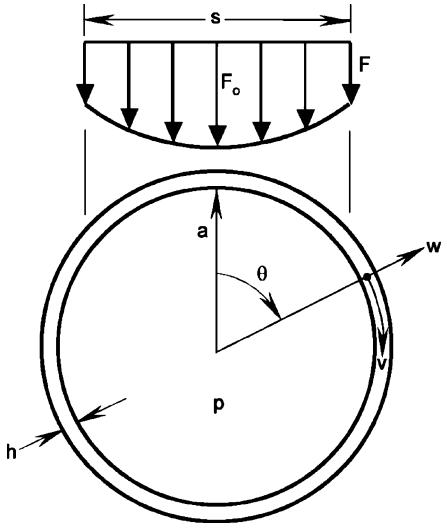

Fig. 1 Notation for evaluation of wall vibrations induced in pressurized cylinder due to pulsed laser beam.

position θ and time t, and define the displacement of the centroid of each arc element from its initial ($t=0$) position. Variations of w and v in the axial direction are ignored. This is consistent with the neglect of end wall effects (i.e., the assumption $a/L \ll 1$) and the assumption of a slab beam with a fluence profile that does not vary in the axial direction. Fung et al.[5] have provided momentum conservation equations that describe the oscillations of a pressurized cylinder. These equations represent a generalization, so as to include the effect of internal pressure, of the Love–Timoshenko formulation[6] of the equations of motion for a vibrating thin-walled cylinder. The neglect of axial derivatives in Eqs. (4) of Fung et al.[5] leads to

$$\frac{1}{\omega_0^2}\frac{\partial^2 w}{\partial t^2} = \varepsilon_i\left(\frac{\partial^2 w}{\partial\theta^2} - \frac{\partial v}{\partial\theta}\right) + \frac{1}{12}\left(\frac{h}{a}\right)^2\left(\frac{\partial^3 v}{\partial\theta^3} - \frac{\partial^4 w}{\partial\theta^4}\right) - \left(\frac{\partial v}{\partial\theta} + w\right) \tag{2a}$$

$$\frac{1}{\omega_0^2}\frac{\partial^2 v}{\partial t^2} = \frac{\partial w}{\partial\theta} + \frac{\partial^2 v}{\partial\theta^2} + \frac{1}{12}\left(\frac{h}{a}\right)^2\left(\frac{\partial^2 v}{\partial\theta^2} - \frac{\partial^3 w}{\partial\theta^3}\right) \tag{2b}$$

where

$$\omega_0^2 = [E/(1-\nu^2)](1/(\rho a^2)) = E'/(\rho a^2) \tag{2c}$$

$$\varepsilon_i = \sigma_i[(1-\nu^2)/E] = \sigma_i/E' \tag{2d}$$

Equations (2a) and (2b) are perturbation equations in the sense that they describe departures from the initial pressurized cylinder configuration. These perturbation equations incorporate the assumption that the axial-strain perturbation is zero and represent a plane-strain approximation.[6,7] Here, ν, E, and $E' = E/(1-\nu^2)$ are Poisson's ratio, the modulus of elasticity, and an effective modulus of elasticity, respectively. The quantity ω_0 will be shown to be the fundamental vibration frequency of a pressurized cylinder. The quantity ε_i is a parameter that is related to the initial tensile (hoop) strain induced by the pressurization process. If the separation distance between the end walls is kept constant during the pressurization process, the pressure-induced axial strain is zero, which is consistent with the plane-strain approximation, and ε_i corresponds to the actual pressure induced hoop strain. If the end walls are unconstrained during pressurization, an axial stress $\sigma_i/2$ is induced, and the corresponding pressure-induced hoop strain is $(1-\nu/2)\varepsilon_i/(1-\nu^2)$. In the latter case, the quantity ε_i is viewed as a parameter associated with the plane-strain perturbation equations, which remain applicable subject to the assumption of zero axial-strain perturbations subsequent to the initial pressurization.

Harmonic solutions of Eqs. (2) are now obtained. Assume perturbations of the form

$$w = \sum_{n=0}^{\infty} w_n \cos\, n\theta \sin\omega_n t \tag{3a}$$

$$v = \sum_{n=0}^{\infty} v_n \sin\, n\theta \sin\omega_n t \tag{3b}$$

where n is the vibrational mode number, which, for each mode, equals the number of sine waves around the cylinder circumference. Substitution of Eqs. (3) into Eqs. (2) yields

$$\frac{2(\omega_n/\omega_0)^2}{k_3 + n^2 k_2} = 1 \pm \left[1 - \frac{4n^2(k_2k_3 - k_1k_4)}{\left(k_3 + n^2k_2\right)^2}\right]^{\frac{1}{2}} \tag{4a}$$

$$\frac{v_n}{w_n} = \frac{nk_4}{(\omega_n/\omega_0)^2 - n^2k_2} \tag{4b}$$

where

$$k_1 = 1 + \varepsilon_i + (1/12)(h/a)^2 n^2 \tag{5a}$$

$$k_2 = 1 + (1/12)(h/a)^2 \tag{5b}$$

$$k_3 = 1 + \varepsilon_i n^2 + (1/12)(h/a)^2 n^4 \tag{5c}$$

$$k_4 = 1 + (1/12)(h/a)^2 n^2 \tag{5d}$$

In the limit of zero internal pressure, Eq. (4a) agrees with the frequency expression in Ref. 6 associated with the plane-strain Love–Timoshenko formulation of the equations of motion. Hence, Eq. (4) can be viewed as a generalization of the Love–Timoshenko result for resonant frequency so as to include the effect of internal pressure.

Simplified equations for the frequency and velocity ratio associated with the positive and negative roots of Eq. (4a) are now given. We make the realistic assumptions

$$\varepsilon_i \ll 1, \qquad [(1+N^2)/12](h/a)^2 \ll 1 \tag{6}$$

where N is the value of n, which characterizes the number of active vibrational modes for given boundary conditions and is discussed further in the section following Eq. (9). If terms that are small, compared with one, are neglected, the dependent variables associated with the positive root of Eq. (4a) become

$$\left(\omega_n^+/\omega_0\right)^2 = 1 + n^2 \tag{7a}$$

$$v_n^+/w_n^+ = n \tag{7b}$$

$$\varepsilon_n^+ = \left(w_n^+/a\right)(1+n^2)\cos\, n\theta \sin\omega_n^+ t + \mathcal{O}\left[\left(w_n^+/a\right)^2\right] \tag{7c}$$

where ε_n^+, obtained from Eq. (A2) in Appendix A, is the local hoop strain associated with ω_n^+. The hoop strain ε_n^+ has a linear dependence on w_n^+/a, and ω_n^+ is termed an extensional vibration.[6,8] Equation (7a) indicates that ω_0 equals ω_0^+, the fundamental frequency of the ω_n^+ mode.

Similarly, the dependent variables associated with the negative root of Eq. (4a) become

$$\left(\frac{\omega_n^-}{\omega_0}\right)^2 = \frac{n^2(n^2-1)\left[\varepsilon_i + \dfrac{n^2-1}{12}\left(\dfrac{h}{a}\right)^2\right]}{1+n^2} \tag{8a}$$

$$\frac{v_n^-}{w_n^-} = -\frac{1}{n} \tag{8b}$$

$$\varepsilon_n^- = \frac{1}{2}\left(\frac{w_n^-}{a}\right)^2 (n^2\sin^2 n\theta - 2\cos^2\, n\theta)\sin^2\omega_n^- t \tag{8c}$$

where ε_n^- is the hoop strain associated with ω_n^-. In view of the quadratic dependence of ε_n^- on w_n^-/a, ω_n^- is termed an "inextensional" vibration.[6,8] Note that $\omega_n^- = 0$ for $n = 0, 1$.

In the limit of large n, namely, $1/n \ll 1$, Eqs. (8) become

$$\left(\omega_n^- \big/ \omega_0\right)^2 = n^2\left[\varepsilon_i + (n^2/12)(h/a)^2\right] \tag{9a}$$

$$v_n^- \big/ w_n^- \ll 1 \tag{9b}$$

These are the equations that describe the fundamental vibration mode for a flat plate of width $\pi a/n$. This is a consequence of the fact that, for large n, the arc length between radial velocity nodes, namely, $\pi a/n$, is small compared to the cylinder radius a and thus departs only slightly from a flat plate.

We assume that the internodal distance $\pi a/N$, for the characteristic mode N, is of the order of the laser-beam width s. It follows that an estimate for the value of N, which characterizes the number of active vibrational modes, is

$$N = \mathrm{INT}(\pi a/s) \tag{10}$$

where INT denotes the integer associated with $\pi a/s$. The second inequality in Eq. (6) is then of order $(h/s)^2$. This inequality is satisfied, provided h/s is small, which provides a laser-beam width limitation for the present model. A more accurate method of confirming that the second inequality in Eq. (6) is satisfied is to examine the results of a particular computation.

It is noted in Ref. 9 that, to date, there is no universally accepted formulation of the equations of motion describing oscillations of a thin-walled cylinder. It is also noted in Ref. 9, however, that from the point of view of accuracy there is little difference among these theories. The various formulations that have been proposed differ primarily in the role of the thickness parameter $k = (h/a)^2/12$. Reference 6 discusses nine separate formulations of the equations of motion for an unpressurized thin-walled cylinder of infinite axial extent (i.e., Love–Timoshenko, Flugge, Sanders, Vlasov, Goldenveizer–Novozhilov, Arnold–Warburton, Bienzeno–Grammel, Reissner–Naghdi–Berry, and Epstein–Kennard formulations). If terms involving k^2 are neglected, five of these formulations give the same expression for resonant frequencies as is obtained from the Love–Timoshenko formulation, which is the basis of the present study. If it is further assumed that $(1 + N^2)k \ll 1$, as is done in Eq. (6), then all formulations give the same result for resonant frequencies, which is the result usually quoted in handbooks.[8] The latter result is the same as that given by Eqs. (7) and (8), with $\varepsilon_i = 0$. Thus, Eqs. (7) and (8) generalize the classical result to include the effect of internal pressure. In the present limit of small $(1 + N^2)k$, there does not appear to be any controversy regarding the appropriate choice of the equations of motion.

III. Applications

We now investigate the strain perturbation induced by an energetic laser pulse incident on the cylinder surface. A slab beam is assumed, namely, a beam with uniform width and infinite axial extent. It is further assumed that ablation blowoff creates an impulsive load that results in inward momentum of the cylinder surface. The resulting strain perturbation is determined. The assumption of an impulsive load at $t = 0$ is valid provided that the time interval corresponding to the laser pulse plus wall ablation blowoff is short compared with $\frac{1}{4}$ of the initial vibration cycle.

A. General Solution

Consider the case of a laser pulse of fluence F and width s (Fig. 1) incident on the cylinder surface at time $t = 0$. Let C represent the coupling coefficient, namely, the ratio of the induced impulse (radial momentum/area) to the incident fluence (energy/area). The initial conditions regarding cylinder surface motion are then, for $t = 0^+$,

$$w = v = \frac{\partial v}{\partial t} = 0 \tag{11a}$$

$$\frac{\partial w}{\partial t} = (-1)\frac{CF}{\rho h}\cos\theta, \qquad |\theta| \le \theta_s \tag{11b}$$

$$= 0, \qquad \theta_s < |\theta| \le \pi \tag{11c}$$

where θ_s is the value of θ corresponding to the edge of the laser beam,

$$\theta_s = \sin^{-1}[s/(2a)] \tag{11d}$$

Let F_0 denote the centerline fluence and denote the beam profile by

$$f(\theta) \equiv F/F_0 \tag{12}$$

where $f(\theta)$ is assumed to be symmetric with respect to θ. Conservation of linear momentum indicates that for $t > 0^+$, the center of mass will have a velocity V, in the $\theta = 180$ deg direction, which can be expressed as

$$V = \frac{\text{vertical impulse}}{\text{mass}} = \frac{CF_0}{\pi\rho h}\int_0^{\theta_s} f(\theta)\cos^2\theta\,\mathrm{d}\theta \tag{13a}$$

Equation (13a) assumes that cylinder end-wall mass is negligible and that the cylinder is in space and is unconstrained. The center-of-mass velocity V can be expressed in parametric form as

$$\Phi \equiv \frac{\rho h V}{CF_0} = \frac{1}{\pi}\int_0^{\theta_s} f(\theta)\cos^2\theta\,\mathrm{d}\theta \tag{13b}$$

where Φ equals the fraction of the initial centerline impulse that goes into translation. The perturbations w and v remain small in a coordinate system, which moves with the center of mass. Because Eqs. (2) and (A2) assume small perturbations, we seek solutions in the center-of-mass coordinate system.

We define

$$w_c/a = (CF_0/\rho h)\sqrt{\rho/E'} \ll 1, \qquad \Omega = \omega/\omega_0, \qquad \tau = \omega_0 t \tag{14a}$$

where w_c is a characteristic radial displacement for cases where extensional vibrations characterize local strain. In the latter case, the characteristic frequency is ω_0, the characteristic radial velocity is $CF_0/(\rho h)$, and the characteristic radial displacement w_c is then $CF_0/(\rho h\omega_0)$, which leads to Eq. (14a). The nondimensional frequency Ω and nondimensional time τ are also referenced to the extensional mode. For convenience, we use the notation

$$w \equiv w/w_c, \qquad v \equiv v/w_c \tag{14b}$$

That is, we hence forth use w and v to denote w/w_c and v/w_c, respectively.

The initial conditions, in a coordinate system that moves with the cylinder center of mass, are then

$$w = v = 0 \tag{15}$$

$$(-1)\left(\frac{\partial w}{\partial \tau}\right)_0 = [f(\theta) - \Phi]\cos\theta, \qquad |\theta| \le \theta_s \tag{16a}$$

$$= -\Phi\cos\theta, \qquad \theta_s < |\theta| \le \pi \tag{16b}$$

$$(-1)\left(\frac{\partial v}{\partial \tau}\right)_0 = \Phi\sin\theta, \qquad |\theta| \le \pi \tag{17}$$

A general solution to Eqs. (2) can be expressed in the form

$$w = \sum_{n=0}^{\infty} w_n^{\pm}\cos n\theta\,\sin\Omega_n^{\pm}\tau \tag{18a}$$

$$v = \sum_{n=0}^{\infty} v_n^{\pm}\sin n\theta\,\sin\Omega_n^{\pm}\tau \tag{18b}$$

where, for example,

$$w_n^{\pm}\sin\Omega_n^{\pm}\tau = w_n^{+}\sin\Omega_n^{+}\tau + w_n^{-}\sin\Omega_n^{-}\tau \tag{18c}$$

Recall, from Eqs. (7), (8), and (14a)

$$\left(\Omega_n^{+}\right)^2 = 1+n^2 \tag{19a}$$

$$\left(\Omega_n^{-}\right)^2 = \frac{n^2(n^2-1)}{n^2+1}\left[\varepsilon_i + \frac{n^2-1}{12}\left(\frac{h}{a}\right)^2\right] \tag{19b}$$

$$\frac{v_n^{+}}{w_n^{+}} = n, \qquad \frac{v_n^{-}}{w_n^{-}} = \frac{-1}{n} \tag{19c}$$

Note, from Eqs. (18) and (19b) that

$$\Omega_0^{-} = \Omega_1^{-} = w_0^{-} = w_1^{-} = v_0^{-} = v_1^{-} = 0 \tag{19d}$$

Equations (17), (18b), and (19d) indicate

$$(-1)v_1^{+}\Omega_1^{+} = \Phi, \qquad n=1 \tag{20a}$$

$$(-1)\left(v_n^{+}\Omega_n^{+} + v_n^{-}\Omega_n^{-}\right) = 0, \qquad n\geq 2 \tag{20b}$$

We use a Fourier series to solve for the coefficients in Eq. (18a) subject to Eqs. (16). Let

$$(-1)\left(\frac{\partial w}{\partial \tau}\right)_0 \equiv (-1)\sum_{n=0}^{\infty} w_n^{\pm}\Omega_n^{\pm}\cos n\theta \tag{21a}$$

$$= \frac{a_0}{2} + \sum_{n=1}^{\infty} a_n \cos n\theta \tag{21b}$$

where

$$\pi a_n = \int_{-\pi}^{\pi}(-1)\left(\frac{\partial w}{\partial \tau}\right)_0 \cos n\theta \, \mathrm{d}\theta \tag{22a}$$

or

$$\frac{\pi a_n}{2} = \int_0^{\theta_s} f(\theta)\cos\theta\cos n\theta \, \mathrm{d}\theta, \qquad n\neq 1 \tag{22b}$$

$$= \frac{1}{2}\int_0^{\theta_s} f(\theta)\cos^2\theta \, \mathrm{d}\theta = \frac{\pi\Phi}{2}, \qquad n=1 \tag{22c}$$

Comparing Eqs. (21a) and (21b) and recalling $w_0^{-} = w_1^{-} = 0$ indicates

$$(-1)w_0^{+}\Omega_0^{+} = a_0/2 \tag{23a}$$

$$(-1)w_1^{+}\Omega_1^{+} = a_1 \tag{23b}$$

$$(-1)\left(w_n^{+}\Omega_n^{+} + w_n^{-}\Omega_n^{-}\right) = a_n, \qquad n\geq 2 \tag{23c}$$

The solution of Eqs. (20b) and (23c), subject to Eq. (19c), yields, for $n\geq 2$,

$$w_n^{+}\Omega_n^{+} = w_n^{-}\Omega_n^{-}\big/n^2 = -a_n\big/(1+n^2) \tag{24a}$$

$$v_n^{+}\Omega_n^{+} = (-1)v_n^{-}\Omega_n^{-} = -na_n\big/(1+n^2) \tag{24b}$$

Equation (24a) indicates, for $n\geq 2$,

$$\frac{w_n^{+}}{w_n^{-}} = \frac{(n^2-1)^{\frac{1}{2}}}{n(n^2+1)}\left[\varepsilon_i + \frac{n^2-1}{12}\left(\frac{h}{a}\right)^2\right]^{\frac{1}{2}} \tag{24c}$$

Thus, w_n^{+} is small relative to w_n^{-} for $n\geq 2$. Equations (20a), (23), and (24) provide expressions for the amplitude of each harmonic mode.

In the present notation, the expression for laser-induced strain given by Eq. (A2) becomes

$$\frac{\varepsilon}{w_c/a} = \sum_{n=0}^{\infty}(1+n^2)w_n^{+}\cos n\theta\sin\Omega_n^{+}\tau + \frac{1}{2}\frac{w_c}{a}\left[\left(\sum_{n=2}^{\infty} n w_n^{-}\sin n\theta\sin\Omega_n^{-}\tau\right)^2 - 2\left(\sum_{n=2}^{\infty} w_n^{-}\cos n\theta\sin\Omega_n^{-}\tau\right)^2\right] \tag{25}$$

Terms involving w_n^{+} are small compared with w_n^{-} in the quadratic summation in Eq. (25) and have been neglected therein. The laser-induced strain is a function of $s/2a$, w_c/a, ε_i, and h/a. The normalized strain $\varepsilon/(w_c/a)$ can be viewed as dependent upon the parameters $s/2a$, $w_c/(a\varepsilon_i)$, and $(h/s)^2/\varepsilon_i$. Laser-induced strain is evaluated in the following section for the case of a laser beam with a uniform fluence profile. A Gaussian profile is considered in Appendix B. Emphasis is placed on laser-beam width and cylinder pressure effects.

B. Uniform Beam

We now consider an incident beam with uniform fluence. In this case, $f(\theta)=1$ and, from Eqs. (13) and (22),

$$4\pi\Phi = 2\theta_s + \sin 2\theta_s \tag{26a}$$

$$a_n = \Phi, \qquad n=1 \tag{26b}$$

$$= \frac{1}{\pi}\left(\frac{\sin(n-1)\theta_s}{n-1} + \frac{\sin(n+1)\theta_s}{n+1}\right), \qquad n\neq 1 \tag{26c}$$

The induced strain is evaluated for $s/2a = \mathcal{O}(1)$ and $s/2a \ll 1$. The assumption of a uniform beam implies a discontinuity in laser-induced radial velocity at $\theta=\theta_s$ for cases where $\theta_s < \pi/2$. The present results are applicable for those cases where the uniform beam profile is assumed to have, at its edges, a narrow transition region from finite to zero fluence.

1. *Case $s/2a = \mathcal{O}(1)$*

For $s/2a = \mathcal{O}(1)$, the major contributors to strain are modes with low values of n. We assume that the characteristic laser-induced strain w_c/a is small compared with the characteristic pressure-induced strain ε_i, namely, $w_c/(a\varepsilon_i) \ll 1$. We further assume $(h/s)^2/\varepsilon_i \leq \mathcal{O}(1)$. Equation (25) then becomes

$$\frac{\varepsilon}{w_c/a} = \left[\sum_{n=0}^{\infty}(1+n^2)w_n^{+}\cos n\theta\,\sin\Omega_n^{+}\tau\right]\left[1+\mathcal{O}\left(\frac{w_c}{a\varepsilon_i}\right)\right] \tag{27a}$$

where

$$(-1)(1+n^2)w_n^{+} = (\sin\theta_s)/\pi, \qquad n=0 \tag{27b}$$

$$= \sqrt{2}\Phi, \qquad n=1 \tag{27c}$$

$$= a_n\big/\sqrt{1+n^2}, \qquad n\geq 2 \tag{27d}$$

Equations (27) have been evaluated for $s/2a=1$. The coefficient $(-1)(1+n^2)w_n^{+}$, in Eq. (27a), has the values 0.318, 0.354, 0.095, and -0.010 for $n=0$, 1, 2, and 4. The $n=3, 5, 7, \ldots$ modes have zero amplitude. Clearly, the $n=0$, 1, 2 modes are the major contributors to strain. Numerical results for strain are given in Figs. 2 and 3. The variation of the local strain perturbation $\varepsilon/(w_c/a)$, with angular position θ/π at fixed time $\tau/2\pi$, is indicated in Figs. 2a–2c.

Figure 2a provides the strain variation from time $\tau/2\pi=0$ to the time $\tau/2\pi=0.18$ at which the strain at $\theta/\pi=0$ reaches its minimum value. (Note that a negative value of ε implies a compressive strain perturbation, which is added to the initial pressure-induced tensile strain to find the net local strain.) Figure 2b describes the

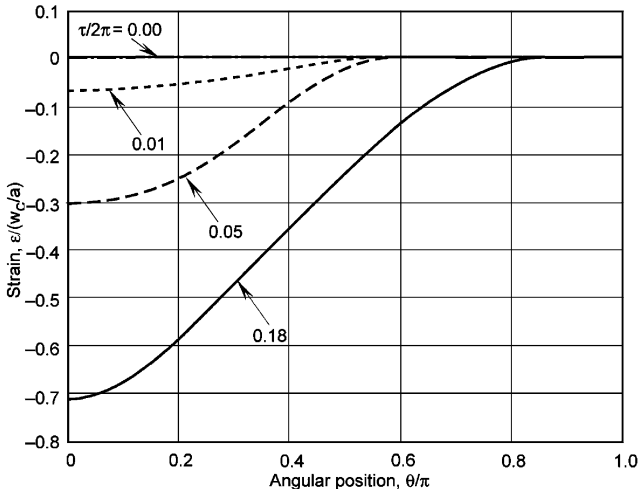

Fig. 2a Variation of laser-induced strain perturbation with angular position at fixed times; case $s/2a = 1$; times $\tau/2\pi = 0.00$–0.18.

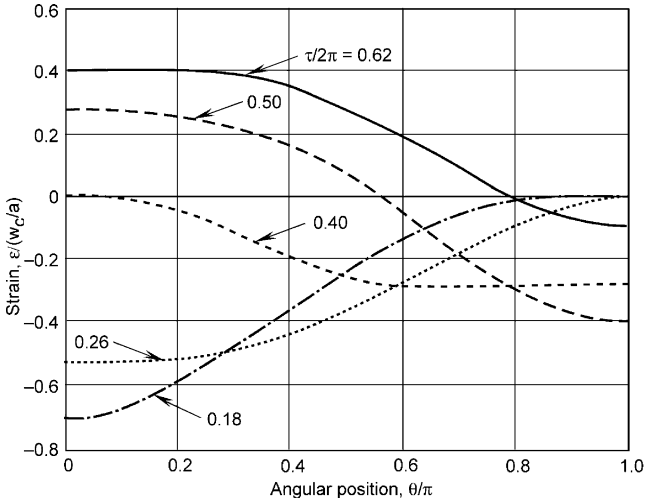

Fig. 2b Variation of laser-induced strain perturbation with angular position at fixed times; case $s/2a = 1$; times $\tau/2\pi = 0.18$–0.62.

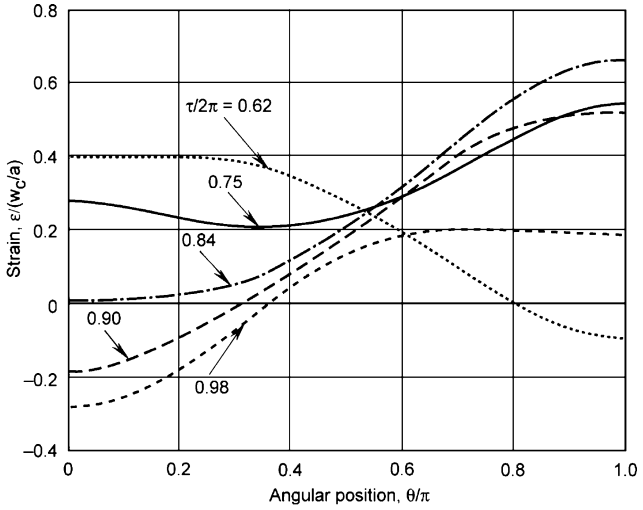

Fig. 2c Variation of laser-induced strain perturbation with angular position at fixed times; case $s/2a = 1$; times $\tau/2\pi = 0.62$–0.98.

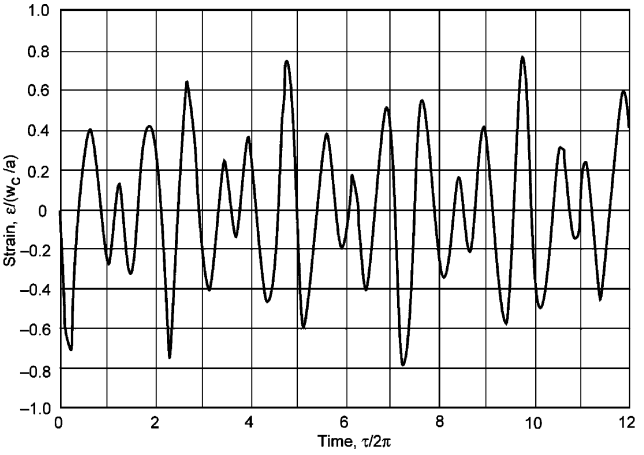

Fig. 3a Variation of laser-induced strain perturbation with time at fixed cylinder location; case $s/2a = 1.0$; location $\theta/\pi = 0.0$.

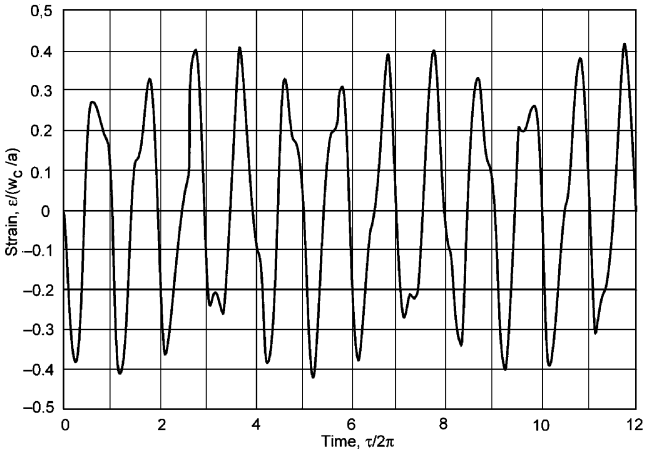

Fig. 3b Variation of laser-induced strain perturbation with time at fixed cylinder location; case $s/2a = 1.0$; location $\theta/\pi = 0.5$.

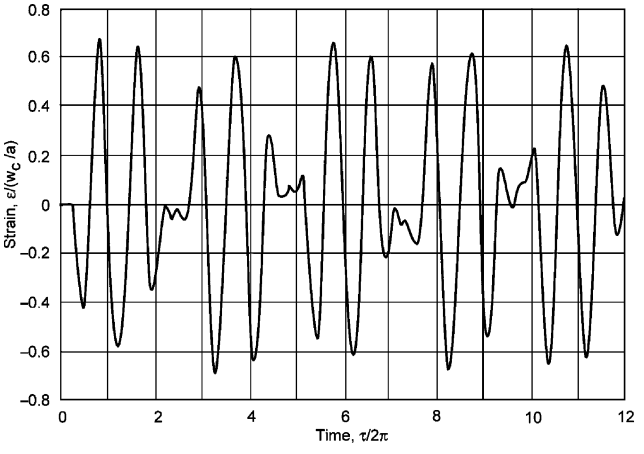

Fig. 3c Variation of laser-induced strain perturbation with time at fixed cylinder location; case $s/2a = 1.0$; location $\theta/\pi = 1.0$.

strain from times $\tau/2\pi = 0.18$ to 0.62, which correspond to the minimum and maximum strain, respectively, at $\theta/\pi = 0$. It is seen from Figs. 2a and 2b that the strain perturbation does not reach $\theta/\pi = 1.0$ until $\tau/2\pi = 0.26$. Figure 2c then follows the strain from $\tau/2\pi = 0.62$ to 0.98. The latter time represents the second minimum at $\theta/\pi = 0$. The time $\tau/2\pi = 0.82$ corresponds to the first maximum strain at $\theta/\pi = 1.0$. The time for the first complete cycle, at $\theta/\pi = 0$, is about $\tau/2\pi = 0.84$, as is expected from the normalization in Eq. (14a). For the present case, the variation of radial

displacement w/a with θ is similar to the hoop strain variation, as can be seen from Eq. (7c).

The variation of the strain perturbation parameter with time, at a fixed location, is given in Figs. 3a–3c.

Figure 3a presents the variation of the strain perturbation parameter with time at $\theta/\pi = 0$. At this location, as already noted, the first maximum occurs at $\tau/2\pi = 0.62$ and has the value 0.402. The largest value of the strain parameter occurs at $\tau/2\pi = 9.73$ and equals 0.769. At this time, the $n = 0$, 1, and 2 modes are essentially in phase. (Note that the sum of the amplitude terms for the $n = 0$, 1, 2 modes is 0.767.) The strain variation at $\theta/\pi = 0.5$ and 1.0 is given in Figs. 3b and 3c. The largest values of the strain parameter at $\theta/\pi = 1.0$ have a magnitude of about 0.6 and are comparable to those at $\theta/\pi = 0$. The largest values of the strain parameter at $\theta/\pi = 0.5$ are about 0.4. Thus, the maximum strain amplitudes decrease in going from $\theta/\pi = 0$ to 0.5 and increase in going from $\theta/\pi = 0.5$ to 1.

Maximum values of the induced strain, at $\theta/\pi = 0$, for $s/2a = 1.0$, 0.8, 0.6, 0.4, and 0.2, are denoted ε_m and are given in Table 1. The values of $\tau/2\pi$, and cycle number, in Table 1 correspond to the $s/2a = 1.0$ case and are approximate for the other cases. Cycles with lower maxima have been omitted. The maximum values of induced strain decrease with decrease in $s/2a$, but not as rapidly as the energy content per unit axial distance $F_0 s$ of the laser beam. Corresponding results for a Gaussian profile laser beam are given in Table B1.

The maximum strain at $\theta = 0$ has a linear dependence on $s/2a$ for small values of $s/2a$, namely,

$$\varepsilon_m/(w_c/a) = 1.194(s/2a)[1 + \mathcal{O}(s/2a)^2] \tag{28}$$

Equation (28) was deduced from numerical solutions. The linear term in Eq. (25) is a function only of $s/2a$. Hence Table 1 and Eq. (28) provide estimates of the contribution of the linear term, towards net laser-induced strain at $\theta = 0$, for all values of $s/2a$, $w_c/(a\varepsilon_i)$, and $(h/s)^2/\varepsilon_i$.

2. Case $s/2a \ll 1$

In the present limit it is expected that mode numbers of order $N \gg 1$ [Eq. (10)] will dominate the vibration. We assume that $N \gg 1$, that Eq. (6) remains satisfied, and, for convenience, that $(h/s)^2/\varepsilon_i \ll 1$. We further assume, to be verified later, that the linear term in Eq. (25) makes a negligible contribution to laser-induced strain. Equation (25) then becomes

$$\frac{2\varepsilon/\varepsilon_i}{[w_c/(a\varepsilon_i)]^2} = \left[\sum_{n=2}^{\infty} a_n \sin n\theta \sin n\sqrt{\varepsilon_i}\tau\right]^2 \tag{29}$$

It is expected that the maximum induced strain will occur at early times at the edge of the incident beam $|\theta| = \theta_s$. Equation (29) was evaluated to determine this maximum strain for the cases $\theta_s = 0.01$, 0.05, 0.10, 0.15, and 0.20. The results are given in Table 2. In each case, the maximum strain occurs at $|\theta| = \sqrt{\varepsilon_i}\tau = \theta_s$.

Table 1 Maximum induced strain at $\theta = 0$, per vibration cycle, for case of uniform beam [see Eq. (27)]

		$\varepsilon_m/(w_c/a)$				
Cycle	$\tau/2\pi$	$s/2a = 1.0$	$s/2a = 0.8$	$s/2a = 0.6$	$s/2a = 0.4$	$s/2a = 0.2$
1	0.62	0.402	0.322	0.242	0.161	0.081
3	1.88	0.415	0.379	0.292	0.198	0.100
4	2.65	0.648	0.558	0.437	0.299	0.152
6	3.95	0.372	0.385	0.328	0.235	0.187
7	4.77	0.743	0.670	0.538	0.374	0.192
8	5.61	0.378	0.363	0.310	0.224	0.118
10	6.87	0.517	0.469	0.368	0.245	0.126
11	7.60	0.551	0.483	0.401	0.292	0.154
13	8.89	0.412	0.392	0.307	0.217	0.112
14	9.73	0.769	0.734	0.622	0.450	0.235
15	10.55	0.318	0.297	0.283	0.223	0.123
17	11.85	0.598	0.556	0.458	0.333	0.175

Table 2 Maximum induced strain for case of uniform beam, $(h/s)^2/\varepsilon_i$ and $s/2a \ll 1$ [see Eq. (29)]

θ_s	θ	$\sqrt{\varepsilon_i}\tau$	$\dfrac{2\varepsilon_m/\varepsilon_i}{(w_c/a\varepsilon_i)^2}$
0.01	0.01	0.01	0.2500
0.05	0.05	0.05	0.2499
0.10	0.10	0.10	0.2494
0.15	0.15	0.15	0.2479
0.20	0.20	0.20	0.2451

Equation (29) can be evaluated analytically in the present limit. For $s/2a \ll 1$,

$$a_n = (2/\pi)(\sin n\theta_s/n) \tag{30}$$

Evaluation of Eq. (29) at $\theta = \sqrt{\varepsilon_i}\tau = \theta_s$ then yields

$$\frac{2\varepsilon_m/\varepsilon_i}{[w_c/(a\varepsilon_i)]^2} = \frac{4}{\pi^2}\left(\sum_{n=1}^{\infty}\frac{\sin^3 n\theta_s}{n} - \sin^3\theta_s\right)^2 \tag{31a}$$

$$= \frac{1}{4}\left(1 - \frac{4}{\pi}\sin^3\theta_s\right)^2 \tag{31b}$$

where Eqs. (1.321-2) and (1.441-1) in Ref. 10 have been used. Equation (31b) is in agreement with the numerical summation of Eq. (29) to within four significant figures for $s/2a \le 0.2$. The assumption that the linear term is negligible in Eq. (25) is valid provided $\psi \gg 1$, as discussed in Sec. V.

IV. Comparison with Reference 2

Although not identified as such, Ref. 2 uses flat-plate expressions to compute the maximum strain induced in a pressurized cylinder by a uniform profile slab beam for both the $s/2a = 1$ and $s/2a \ll 1$ cases. Thickness effects were ignored. We now compare the Ref. 2 results with those of the present model.

For the case $s/2a = 1$, Ref. 2 assumes that the major contribution to strain comes from the $n = 2$ inextensional mode. The corresponding maximum strain occurs at $|\theta| = \pi/4$, $3\pi/4$ and equals

$$(\varepsilon_m/\varepsilon_i)_{\text{Ref 2}} = [2/(3\pi)^2](CF_0/(pa))^2(E'/\rho) \tag{32}$$

which is obtained from the quadratic term in Eq. (A2). From Table 1, the present solution indicates that the maximum strain is associated with the extensional mode, occurs at $\theta = 0$ deg, and equals

$$\varepsilon_m/\varepsilon_i = 0.769(CF_0/(pa))\sqrt{E'/\rho} \tag{33}$$

which is obtained from the linear term in Eq. (A2). Comparison of the fluence required to achieve a given maximum strain yields

$$\frac{(F_0)_{\text{Ref 2}}}{F_0} = \frac{5.12}{\sqrt{\varepsilon_m/\varepsilon_i}} \tag{34a}$$

$$= 51.2, \qquad \varepsilon_m/\varepsilon_i = 0.01 \tag{34b}$$

$$= 16.2, \qquad \varepsilon_m/\varepsilon_i = 0.1 \tag{34c}$$

Thus, for $s/2a = 1$, Ref. 2 overpredicts, by an order of magnitude, the fluence required to achieve a given maximum strain for cases wherein $\varepsilon_m/\varepsilon_i \ll 1$.

In the case $s/2a \ll 1$, the flat-plate model used in Ref. 2 is applicable. A large number of modes, of the order of $N = \pi a/s$, contribute to the maximum strain. However, Ref. 2 states, incorrectly, that the $n = 2$ mode is the "dominant" contributor to the maximum strain and can be used as a "surrogate" for evaluating maximum strain in system studies. Reference 2 concludes that the maximum strain again occurs at $|\theta| = \pi/4$, $3\pi/4$ and has the value

$$(\varepsilon_m/\varepsilon_i)_{\text{Ref 2}} = \tfrac{1}{2}(s/\pi a)^2(CF_0/(pa))^2(E'/\rho) \tag{35}$$

The present theory indicates, from Eq. (31),

$$\varepsilon_m/\varepsilon_i = \tfrac{1}{8}(CF_0/(pa))^2(E'/\rho) \tag{36}$$

Comparison of the fluence required to provide a given maximum strain yields

$$\frac{(F_0)_{\text{Ref 2}}}{F_0} = \frac{\pi/4}{s/2a} \tag{37a}$$

$$= 78.5, \qquad s/2a = 0.01 \tag{37b}$$

$$= 7.85, \qquad s/2a = 0.1 \tag{37c}$$

In the present limit, $s/2a \ll 1$, Ref. 2 again overstates the required fluence by an order of magnitude as well as mislocating the maximum strain region.

V. Beam Width and Cylinder Pressure Effect

The effect of laser-beam width, via parameter $s/2a$, and cylinder internal pressure, via parameter $w_c/(a\varepsilon_i)$, on the relative magnitude of the linear and quadratic terms in Eq. (25) is now investigated subject to the assumption that $(h/s)^2/\varepsilon_i \ll 1$.

The maximum strain associated with the quadratic term in Eq. (25) is denoted by subscript qu, and, for $(h/s)^2/\varepsilon_i \ll 1$, can be expressed as

$$\frac{2(\varepsilon_m/\varepsilon_i)_{\text{qu}}}{[w_c/(a\varepsilon_i)]^2} = \frac{64}{135\pi^2} = 0.0480, \qquad \frac{s}{2a} = 1 \tag{38a}$$

$$= 0.250, \qquad \frac{s}{2a} \ll 1 \tag{38b}$$

Equation (38a) corresponds to the maximum value of the quadratic term at $\theta = \pi/4$ for the $n = 2$ mode and is within a few percent of the maximum value associated with all of the modes. Equation (38b) follows from Eq. (31).

The maximum strain associated with the linear term in Eq. (25) is denoted by subscript li and can be expressed as

$$\frac{(\varepsilon_m/\varepsilon_i)_{\text{li}}}{w_c/(a\varepsilon_i)} = 0.769, \qquad \frac{s}{2a} = 1 \tag{39a}$$

$$= 1.194\frac{s}{2a}, \qquad \frac{s}{2a} \ll 1 \tag{39b}$$

which follows from Table 1 and Eq. (28).

Let ψ denote the ratio of the maximum value of the quadratic strain term to the maximum value of the linear strain term in Eq. (25) for given values of $s/2a$ and $w_c/(a\varepsilon_i)$. Utilizing Eqs. (38) and (39), and again assuming $(h/s)^2/\varepsilon_i \ll 1$, ψ can be approximated by

$$\psi \equiv (\varepsilon_m)_{\text{qu}}/(\varepsilon_m)_{\text{li}} \tag{40a}$$

$$\approx 0.06(w_c/(a\varepsilon_i))(2a/s) \tag{40b}$$

where the coefficient 0.06 is a compromise between the values 0.031 and 0.105 associated with the $s/2a = 1$ and $s/2a \ll 1$ cases. When $\psi \ll 1$, the quadratic term is negligible, and when $\psi \gg 1$ the linear term is negligible in Eq. (25). The values $\psi \ll 1$ and $\psi \gg 1$ correspond to extensional and inextensional vibrations, respectively. These values of ψ also correspond to the cases $s/2a = \mathcal{O}(1)$ and $s/2a \ll 1$, respectively, in Sec. III. When $\psi = \mathcal{O}(1)$, both the linear and the quadratic terms in Eq. (25) contribute to the net strain.

The assumption $(h/s)^2/\varepsilon_i \ll 1$ implies that bending moments are small compared with the tensile stress induced by the internal cylinder pressure. This assumption is violated for cases of negligible (or zero) pressure. In these cases $(h/s)^2$, rather than ε_i, becomes the appropriate normalization parameter.

VI. Conclusions

Vibrations induced in a pressurized cylinder, by a high-energy pulsed laser beam, have been evaluated. The vibrations consist of both extensional and inextensional modes. The strain induced by these modes has a linear and a quadratic dependence on vibration amplitude, respectively. Numerical results have been presented for the case of a pressurized cylinder, uniform and Gaussian beams, and $s/2a = \mathcal{O}(1)$. In this case, the vibration is extensional, and the induced strain is a linear function of vibrational amplitude. With decrease in pressure, or beam width, inextensional vibrations become important. In the limit $s/2a \ll 1$, the vibration is inextensional, and the induced strain has a quadratic dependence on vibration amplitude. Numerical results for strain, in the case $s/2a \ll 1$, have also been presented. Equation (25) can be used to evaluate induced strain for cases where both the extensional and inextensional contributions are important. The role of pressure level and laser beam width in determining the relative importance of the linear and the quadratic terms in Eq. (25) is defined by the parameter ψ introduced in Sec. V.

The present study provides a simplified model of laser-induced strain, in pressurized cylinders, by virtue of the assumptions of both a slab beam and a cylinder of infinite axial extent. The effect of end walls and beams with circular cross sections requires further study.

Appendix A: Stress and Strain Expressions

Strain is related to the perturbations v, w in the following section. Let $a\Delta\theta$ denote an elementary arc section. The strain induced by a displacement can be expressed (Fig. A1) as

$$[(1+\varepsilon)a\Delta\theta]^2 = (\Delta w)^2 + \left[(a+w)\Delta\theta + \frac{\partial v}{\partial\theta}\Delta\theta\left(1+\frac{w}{a}\right)\right]^2 \tag{A1}$$

Expansion, retention of leading terms, and application of the limit $\Delta\theta \to 0$ indicates

$$\varepsilon = \frac{w}{a} + \frac{\partial v}{a\partial\theta} + \frac{1}{2}\left(\frac{\partial w}{a\partial\theta}\right)^2 + \frac{w}{a^2}\frac{\partial v}{\partial\theta} \tag{A2}$$

which agrees with Eq. (9.7.21) in Ref. 9.

Equation (A2) defines the laser-induced hoop strain along the midsection of the cylinder wall. Within the plane-strain approximation, the corresponding hoop stress perturbation is $\sigma = \varepsilon E'$. The net hoop stress is then $\sigma_i + \sigma$.

Appendix B: Gaussian Beam

The maximum strain induced by a slab laser beam with a Gaussian fluence profile is now evaluated. The profile is expressed as

$$F/F_0 = \exp[-2(2y/s)^2] \tag{B1a}$$

where y is the transverse coordinate and s equals the characteristic full beam width. The net beam energy, per unit axial length, is

$$E = \int_{-\infty}^{\infty} F\,\mathrm{d}y = \sqrt{\frac{\pi}{8}}sF_0 \tag{B1b}$$

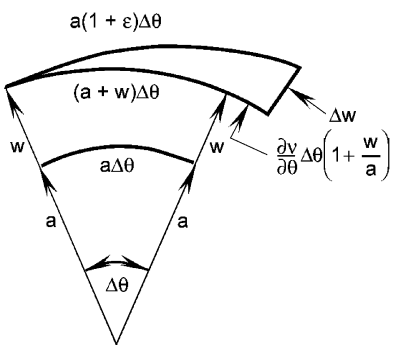

Fig. A1 Notation used for evaluation of strain ε.

Note that

$$2y/s = (2a/s)\sin\theta \tag{B1c}$$

The Fourier coefficients are found from

$$\frac{\pi a_n}{2} = \int_0^{\pi/2} \exp\left[-2\left(\frac{\sin\theta}{s/2a}\right)^2\right]\cos\theta\cos n\theta\,\mathrm{d}\theta, \qquad n \neq 1 \tag{B2a}$$

$$= \frac{1}{2}\int_0^{\pi/2} \exp\left[-2\left(\frac{\sin\theta}{s/2a}\right)^2\right]\cos^2\theta\,\mathrm{d}\theta, \qquad n = 1 \tag{B2b}$$

These have been evaluated using numerical integration. Substitution into Eq. (27a) has yielded the maximum strain at $\theta = 0$. The results are given in Table B1 and can be compared to the results for a uniform profile beam given in Table 1. In both cases, the time at which the maximum strain occurs, for each cycle, is approximately the same. The magnitude of the maximum strain parameter is smaller, for the Gaussian beam, as is expected from physical considerations. However, for a given energy and beam width, the Gaussian profile generates a larger maximum strain. For $s/2a = \mathcal{O}(1)$, Table B1 provides the maximum strain on the cylinder. When $s/2a \ll 1$, the maximum strain can be estimated from Eq. (29).

Table B1 Maximum induced strain at $\theta = 0$, per vibration cycle, for the case of a Gaussian beam [see Eq. (27)]

		$\varepsilon_m/(w_c/a)$				
Cycle	$\tau/2\pi$	$s/2a = 1.0$	$s/2a = 0.8$	$s/2a = 0.6$	$s/2a = 0.4$	$s/2a = 0.2$
1	0.62	0.241	0.199	0.151	0.101	0.050
3	1.84	0.273	0.234	0.183	0.124	0.063
4	2.64	0.418	0.355	0.276	0.188	0.095
6	3.99	0.263	0.230	0.196	0.171	0.124
7	4.77	0.505	0.434	0.343	0.236	0.121
8	5.62	0.280	0.247	0.202	0.143	0.074
10	6.90	0.333	0.285	0.224	0.154	0.079
11	7.56	0.362	0.318	0.260	0.186	0.097
13	8.87	0.284	0.246	0.197	0.137	0.070
14	9.72	0.564	0.497	0.405	0.286	0.148
15	10.60	0.243	0.224	0.194	0.145	0.078
17	11.89	0.418	0.367	0.299	0.212	0.110

Acknowledgments

This work was funded under Air Force Contract F04701-00-C-0009. The authors are indebted to Dick J. Chang, Michael J. O'Brien, and Keith P. Zondervan of The Aerospace Corporation for constructive comments during the course of this study.

References

[1]American Physical Society Study, "Science and Technology of Directed Weapons," *Reviews of Modern Physics*, Vol. 59, No. 3, Pt. 2, 1987, pp. S33, S128–S140.

[2]Sutton, G. W., "High-Energy Single-Pulse Laser Structural Damage of Cylindrical Shells," AIAA Paper 2001-8-7, July 2001.

[3]Mirels, H., and Zondervan, K. L., "Vibration of Pressurized Thin-Walled Cylinder Induced by Pulsed Laser," AIAA Paper 2002-8-5, July–Aug. 2002.

[4]Mirels, H., and Zondervan, K. L., "Vibration of Pressurized Thin-Walled Cylinder Induced by Pulsed Laser—Addendum," The Aerospace Corp., Aerospace Rept. TOR-2002(1019)-1, El Segundo, CA, Aug. 2002.

[5]Fung, Y. C., Sechler, E. E., and Kaplan, A., "On the Vibration of Thin Cylindrical Shells Under Internal Pressure," *Journal of Aeronautical Sciences*, Vol. 24, No. 9, 1957, pp. 650–660.

[6]Leissa, A. W., "Vibration of Shells," NASA SP-288, 1973.

[7]Sokolnikoff, I. S., *Mathematical Theory of Elasticity*, McGraw–Hill, New York, 1956, p. 250.

[8]Flugge, W., *Handbook of Engineering Mechanics*, McGraw–Hill, New York, 1962, pp. 61-25–61-27.

[9]Nayfeh, A. H., and Pai, P. F., *Linear and Nonlinear Structural Mechanics*, Wiley, New York, 2004, pp. 560, 613, 630–641.

[10]Gradshteyn, I. S., and Ryzhik, I. M., *Table of Integrals, Series, and Products*, Academic Press, New York, 1980, pp. 26, 38.

B. Balachandran
Associate Editor